SEMARAK ILMU PUBLISHING

Journal of Advanced Research in Fluid Mechanics and Thermal Sciences

Journal homepage:
https://semarakilmu.com.my/journals/index.php/applied_sciences_eng_tech/index
ISSN: 2462-1943

Cylindrical Dielectric Resonator as Dielectric Matching on Microwave Amplifier for the Unconditionally Stable and Conditionally Stable Transistor at 5 GHz Frequency

Rashidah Che Yob[1,*], Nor Muzlifah Mahyuddin[2], Mohd Fadzil Ain[2], Mohd Aminuddin Jamlos[1], Nur Hidayah Ramli[1], Norfatihah Bahari[1], Mohd Wafi Nasrudin[3], Liyana Zahid[1]

[1] Faculty of Electronic Engineering and Technology, Universiti Malaysia Perlis, Perlis, Malaysia
[2] School of Electrical and Electronic Engineering, Engineering Campus, Universiti Sains Malaysia, Penang, Malaysia
[3] Advanced Computing, Centre of Excellent, Universiti Malaysia Perlis, Perlis, Malaysia

ARTICLE INFO

Article history:
Received 6 October 2022
Received in revised form 16 December 2022
Accepted 20 December 2022
Available online 28 December 2022

Keywords:
Amplifier, Cylindrical Dielectric Resonator, Microwave Systems, Stability Performances

ABSTRACT

Stability and matching techniques on microwave amplifier have been an important consideration to maintain their required performances, but typically its frequency dependent. Thus, a frequency variable mechanism is required. The dielectric matching employing the stability and matching techniques on microwave amplifier with cylindrical dielectric resonator has been investigated and realized. The cylindrical dielectric resonator (CDR) with parallel microstrip lines is proposed at 5 GHz frequency for unconditionally stable and conditionally stable transistor as dielectric matching. Hence, the proposed dielectric resonator with +2 mm spacing and 155˚ of curved configuration indicated the best performances for preliminary study. The result improves the performance of the parallel inhomogeneous CDR by 9.77%. Subsequently, the homogeneous CDR is also successfully working as the variable frequency mechanism for unconditionally stable and conditionally stable transistor at 5 GHz frequency in maintaining their stability performances.

1. Introduction

One of the solutions to improve the accuracy and acquire most performances for the microwave amplifier is generally, represented by the stability element and matching techniques. Although, it depends on the specific circuit requirements such as the simplicity in practical realization, the frequency bandwidth, the least noise figure, design implementation and adaptability, stable operations conditions, and linearity. Thus, many types of stability and matching networks are available [1-5], which include lumped element [5], transmission lines [6], and variable matching network [7-11]. The qualitative summary of the stability and matching techniques for microwave amplifier of the earlier research done are listed and summarized in Table 1.

* *Corresponding author.*
E-mail address: rashidahcheyob@unimap.edu.my

https://doi.org/10.37934/araset.29.1.3045

Table 1
The qualitative summary of the stability and matching techniques for microwave amplifier

Stability & matching networks		**Freq. (GHz)**	**Amplifier topologies**	**Considerations**	**Performances**	**Ref.**
Input	***Output***					
Shunt negative feedback	-	2.4	Low Noise Amplifier (LNA)	• NF • Gain • Power consumption	• NF: 2.9 dB • S_{11}=< -13 dB • Power consumption: 985µW	[5]
-	Tuneable impedance matching (coupled inductors)	0.2-0.3	Power Amplifier (PA)	• Efficiency • Maximum power output.	• A useful option for CMOS design when low-*Q* inductors must be used.	[9]
Narrowband tunable impedance-matching (π-structure with varactors in series with inductors)		1	Low Noise Amplifier (LNA)	• Noise figure (NF). • Tunable matching network.	• Tuned in a 50% BW. • S_{11}=< -20 dB • S_{21}= > -3 dB	[10]
Lumped elements (L-shape: Inductors & Capacitors)		4-8	Low Noise Amplifier (LNA)	• Gain. • NF.	• S_{11}= -50 dB • S_{21}= 13 dB • *NF*= 2.2 dB • *VSWR*=1.5 • *K=1.07*	[12]
Load line matching.		2.5	Power Amplifier (PA)	• Linearity. • Efficiency.	• Maximum efficiency power is 66%.	[13]
Combination L-L matching circuits.		1-10	Low Noise Amplifier (LNA)	• Gain. • Stability factor. • NF.	• S_{21}= 10 dB • S_{12}=-49.59 dB • *NF*= 0 dB	[14]
Feedback resistor for improved stability of the circuit (R = 500Ω). Lumped, distributed and radial stub elements for matching.		10	Low Noise Amplifier (LNA)	• Minimum NF. • High gain.	• S_{11}= -17.35 dB • S_{21}= 14.77 dB • S_{12}=-18 dB • S_{22}=-10.24 dB • *NF*= -0.775 dB	[15]
Lumped, distributed & radial stub elements.		10-15	Low Noise Amplifier (LNA)	• High gain. • Minimum NF.	• S_{11}= -17.15 dB • S_{21}= 14.35 dB • S_{12}=-17.023 dB • S_{22}=-16.92 dB • *NF*= -0.92 dB	[16]
Adaptive (automatic) impedance-matching network (capacitor-matrix)		1.3	Power Amplifier (PA)	• Resonant frequency. • Power transfer efficiency.	• Power transfer efficiency increased up 88% when distances changes 0 to 1.2 m.	[17]
RLC feedback for stabilization. T and L matching network.		6	Low Noise Amplifier (LNA)	• NF. • Gain. • Stability factor.	• S_{11}= -17.2 dB • S_{21}= 14.14 dB • S_{12}=-23.5 dB • S_{22}=-6.29 dB • *NF*= 1.816 dB • *K=1.304*	[18]

Table 1 (cont.)
The qualitative summary of the stability and matching techniques for microwave amplifier

Stability & matching networks		Freq. (GHz)	Amplifier topologies	Considerations	Performances	Ref.
Input	***Output***					
Negative feedback circuit for stabilization. Smith Chart and tuning matching.		2.45	Low Noise Amplifier (LNA)	• Improved sensitivity of the systems. • Maximum gain.	• S_{11} & S_{22} = < - 15 dB • S_{21}= > 15 dB • *NF*= < 0.8 dB	[19]
-	Two variable capacitors	2.14	Power Amplifier (PA)	• Maximum PAE.	• PAE increased by 21.8 % from 33.4% to 55.2 %.	[20]
Smith chart utility		8	Low Noise Amplifier (LNA)	• Gain. • Stability analysis.	• *Gain*=10dB	[21]
Symbolic approach (Heuristic algorithm)-generated design variables values in-terms of these unknowns.		1-3	Low Noise Amplifier (LNA)	• Output power – *maintain the efficiency power at the same maximum level*. • Quality factor, *Q*. • Enhance efficiency.	• S_{11} & S_{22} =< -10 dB • S_{21}= > 10 dB • *NF*= < 1 dB	[22]
Distributed circuits elements (lumped elements matching & numerical optimization techniques)		1-2	Power Amplifier (PA)	• Broadband matching.	• S_{11} =< -20 dB	[23]
RC feedback network (*R*=120 Ω, *C*=1pF)		4	Power Amplifier (PA)	• Global stability analysis. • Effect of stabilization network. • Potential unstable PA.	• Efficient determination of the unstable operation conditions of microwave amplifiers.	[24]
Double feedback technique		5.8	Low Noise Amplifier (LNA)	• Gain improvement. • Minimize noise figure	• S_{11} = -14.354 dB • S_{12}= - 22.465 dB • S_{21}= 20.877 dB • S_{22} = -11.879 dB • *NF*= 0.341 dB • *K* = 1.001	[25]

Based on this related works, the main considerations of the works are highlighted, i.e., gain, stability, and noise factor. However, if the stability issues are not solved, the gain and noise factor will be much affected. As mentioned earlier, the stability factor is influenced by the changes in operating frequency. Some amplifiers can reside in either a stable or unstable region, depending on the operating frequency. External disturbances such as temperature variation can only vary the frequency, thus making the amplifier susceptible to uncertainty in the aspect of stability. Therefore, the operating frequency needs to be easily controlled or tuned for such cases.

The work in [26] explores the use of cylindrical dielectric resonator (CDR) as frequency variable elements. A CDR is a piece of the unmetallized ceramic with a high dielectric constant, in which the electromagnetic fields are confined to the dielectric region, and it is immediate vicinity. The placement of a dielectric resonator with a constant physical characteristic can tune the operating

frequency of the two-way power divider, which improving its performances for multifrequency operation without changing its physical dimensions. The implementation of such DR gives the input return loss better than 20 dB in operation of the divider at multiple frequencies. Besides that, the microstrip line configuration is also another important consideration that can influence the performance of the microwave circuits. The idea is to investigate the microstrip line configuration which is adopted by [27-29]. This microstrip line configuration is represented as coupling configuration between the DR and monolithic microwave integrated circuits (MMICs) in [28] as the new developments to improve high output power [27] and the phase noise [28] of the dielectric resonator oscillator (DRO). In this article, this microstrip line configuration is investigated to explore the frequency changes of the microwave amplifier, where it should be operated at 5 GHz frequency. Meanwhile, the use of the dielectric resonator (DR) as frequency variable elements is a great approach to implement on microwave amplifier to ascertain the frequency of amplifier resides within the stable region. The characteristic of the DR is initially investigated through the multi-permittivity dielectric resonator (MPCDR) or also known as an inhomogeneous DR due to their dual permittivities, which can be served at one time. The uses of the multi-permittivity DR as in [30-32] have overcome the drawbacks of the homogeneous DR, while the basic geometry of the resonator is maintained. Thus, the available theoretical, numerical, and experimental tools can be effectively applied to the proposed DRs.

In [30-32], the MPCDR are represented by high and low permittivity with 90˚ pie-shaped sectors of each permittivity materials that are positioned in non-adjacent quadrants. The high permittivity, ε_{r1} represents by magnesium titanium oxide doped with cobalt ($MgTiO_3$ + Co) of 15 and only $MgTiO_3$ of 15.72 in [30-31] and [32], respectively. The ε_{r1} of DR materials has high Q-factors that stored more of electromagnetic energy inside and helps in achieving a strong coupling to the feeding structure (coupling implementation). Meanwhile, the low permittivity, ε_{r2} is presented by Roger substrate (RT6010) of 10.2 and ($CoTiO_3$) of 9.85 in [32]. The ε_{r2} of DR materials tends to be operated in wider bandwidth (BW). The combination of the high and low permittivity plays an important role in achieving wideband operation with strong coupling coefficients. The strong coupling coefficient gives the most radiation pattern of the electric and magnetic fields. Besides that, the wider BW can handle high data rates, multi-lingual communication, multi-communication channels and control data traffic of the modern communication systems. By referring to [32], the different single and multi-permittivity geometries of CDR are evaluated for wideband performances.

In this work, a CDR with parallel microstrip lines is presented as dielectric matching on the microwave amplifier for unconditionally stable and conditionally stable transistor at 5 GHz frequency. The preliminary study was carried out for the CDR in-terms of spacing distance and curve configuration of parallel microstrip lines and the angular position of the CDR. The results will influence the performance of scattering parameters (S_{11} and S_{21}) and their resonant frequency. The best configuration of the proposed CDR will be incorporated as the dielectric matching for unconditionally stable and conditionally stable transistor at 5 GHz frequency. The prototype homogeneous CDR is represented by Calcium Copper Titanate (CCTO) which is used as dielectric matching on microwave amplifier with the unconditionally stable and conditionally stable transistors. A close agreement between the simulation and experimental results is obtained. In the following section, the DR specification is described, followed by the preliminary study of the DR and then the implementation of the homogeneous DR as dielectric matching on microwave amplifier for stability performances.

2. Specification of Dielectric Resonator

The specification of the DR including the substrate and related parameters, the detail parameters of DR and the microstrip lines dimensions and its characteristics have been discussed in the next following subsection, respectively.

2.1 Substrate RO4003C Series and Related Parameters

The selection of the board material is very important for high operating frequency, which is the C-band frequency at 5 GHz frequency. Hence, the RO4003C substrate is a product by Rogers Corporation has been used for this research. The RO4003C substrate has low dielectric tolerance and low loss [33]. Furthermore, its excellent electrical performance makes it a good choice for applications at high operating frequencies range. Moreover, it also offers a low cost for circuit fabrication. The electrical characteristics of the RO4003C material used in modelling the DR circuit are stated in Table 2 [33].

Table 2
The electrical characteristics of the RO4003C material

Parameters	Symbol	Value
Dielectric constant	ε_r	3.38 ± 0.05
Dissipation factor	tan δ	0.0027
Thermal coefficients of ε_r	°C	+40
Substrate thickness	H	0.813 mm
Copper thickness	T	0.035 mm
Conductor conductivity	σ	5.8 x 10^7 S/m

The wavelength for the dimension of 50 Ω transmission line is calculated using (1), where the dielectric constant, ε_r is 3.38; the operating frequency, f is 5 GHz at the speed of light, c, which gives the value of 8.15 mm for a quarter wavelength.

$$\lambda_g = \frac{c}{\sqrt{\varepsilon_r} f} \quad (1)$$

Meanwhile, the dimension of a substrate with the copper ground plane is summarized in Table 3.

Table 3
The dimensions of a substrate with the copper ground plane

Parameters	Value (mm)
Length, l	32.61
Width, w	30
Height of substrate, h	0.813
Thickness of copper, t	0.035
Substrate material	Duroid (Roger RO3004C)
Grounded material	Copper

2.2 Parameters of Dielectric Resonator

The structure of the DR mainly consists of three basic layers; the bottom layer is copper, followed by the substrate that places the DR above it together with the feeding mechanism, which is a microstrip line. Lastly, the upper layer is filled up with the vacuum to avoid the field radiation in the air or block the noise and interferences. The parametric analysis for the parallel CDR is investigated

for the same waveguide port position. The common parameters of the DR are referred from [29-31], especially their dielectric permittivity of the DR. The inhomogeneous CDR is formed by two different dielectric materials, which are Magnesium Titanate Oxide, ε_{r1}, and Cobalt Titanate Oxide, ε_{r2}, which also known as $MgTiO_3$ (MTO) and $CoTiO_3$ (CTO), respectively. The value of this inhomogeneous CDR of each material is 15.717 and 9.855, respectively [32]. The details parameters and characteristics of the inhomogeneous CDR are calculated using (2) for its diameters, which about 2% in the range of a/L [30,34]. The details of parameters and characteristics of the inhomogeneous CDR are summarized in Table 4.

$$f_{GHz} = \frac{34}{a_{mm}\sqrt{\varepsilon_r}}\left(\frac{a}{L} + 3.45\right) \quad (2)$$

Table 4
The details of parameters and characteristics of the inhomogeneous CDR

Property	Dielectric Permittivity		Loss Tangent		Parameters	
	MTO (ε_{r1})	***CTO (ε_{r2})***	***MTO (tan δ)***	***CTO (tan δ)***	***Thickness***	***Radius***
Value	15.72	9.86	-0.0133	-0.0143	2.5 mm	7.5 mm

Both MTO and CTO as reported in [35] claims that this material is well known as low loss dielectric ceramics and have wide applications in communication systems, especially as base materials to elaborate the resonators, filters, antennas, radars, and global positioning systems that work at microwaves frequencies.

2.3 Microstrip Line Dimensions and Characteristics

In this article, the microstrip line is used as the feeding mechanism for the DR. The parallel microstrip lines produce the optimum power level with more stability that will fulfil the purpose of the DR as the stability elements and matching components in this work. The dimensions of the parallel microstrip lines would be obtained by using (3) until (6) depending on the width to height ratio [4].

For w/h <1,

$$\varepsilon_{eff} = \frac{\varepsilon_r+1}{2} + \frac{\varepsilon_r-1}{2}\left[\left(1+\frac{12h}{w}\right)^{-0.5} + 0.04\left(1-\frac{w}{h}\right)^2\right] \quad (3)$$

$$Z_o = \frac{60}{\sqrt{\varepsilon_{eff}}} ln\left(\frac{8h}{w} + 0.25\frac{w}{h}\right) \quad (4)$$

For w/h >1,

$$\varepsilon_{eff} = \frac{\varepsilon_r+1}{2} + \frac{\varepsilon_r-1}{2}\left(1+\frac{12h}{w}\right)^{-0.5} \quad (5)$$

$$Z_o = \frac{377}{\sqrt{\varepsilon_{eff}\left[\frac{w}{h}+1.393+\left(0.667ln\left(\frac{w}{h}+1.444\right)\right)\right]}} \quad (6)$$

where, h is the substrate thickness, w is the microstrip line width, t is the conductor thickness, ε_{eff} is an effective dielectric constant of the substrate, and ε_r is the dielectric constant of the substrate.

The dimension of parallel microstrip lines is calculated by using the impedance calculation option in CST software, where h is the height of substrates, *eps* is the Epsilon (permittivity) of the substrates and w is the width of the microstrip line to yield 50 Ω line. The length of the parallel microstrip lines is kept to λ/2 which represents the center of the overall size of the substrate. The parameters value

and material of the parallel microstrip lines are summarized in Table 5. Practically, the waveguide port is realized by a SMA connector by providing connectivity to the equipment, which requires coaxial connections.

Table 5
The parameters value and material of the parallel microstrip lines

Parameters	Value (mm)
Length, *l*	λ
Width, *w*	1.898
Thickness of microstrip line, *t*	0.035
Microstrip line material	Copper

3. Preliminary Study of Dielectric Resonator

The preliminary study of the DR is divided into three subsections, which involve the spacing and curves configuration of parallel microstrip lines. This is followed by the orientation of angular position of the dielectric resonator, especially for the multi-permittivity or inhomogeneous CDR. The details about the preliminary study of the DR are presented in this subsection.

3.1 Spacing of Parallel Microstrip Lines

The parametric study is focusing on the different spacing between the parallel microstrip lines first, which known as the coupling coefficient as shown in Figure 1. The suitable spacing between parallel microstrip lines and the CDR needs to be determined. Seven different spacing between the parallel microstrip lines and the CDR is examined for 10 mm (-2.5 mm), 13 mm (-1 mm), 15 mm (0 mm), 17 mm (+1 mm), 19 mm (+2 mm), 21 mm (+3 mm) and 25 mm (+ 5 mm). The references for the spacing between the parallel microstrip lines are at 15 mm (0 mm). Theoretically, the return loss, S_{11} at the input port should be below 10 dB, which means that 90 % of the input power is successfully delivered, and reflected power is around 10 % [4]. The findings of this investigation are summarized in Table 6.

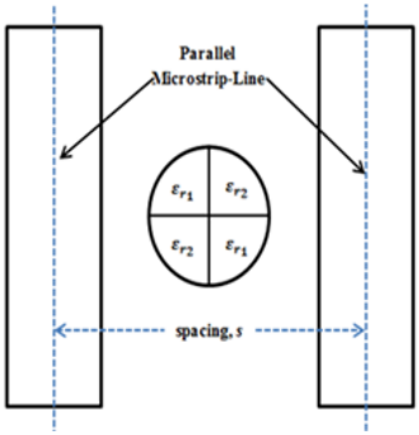

Fig. 1. Parametric study of the different spacing between the parallel microstrip lines

The obtained S-parameters responses (S_{11} and S_{21}) for different spacing between the parallel microstrip lines and the CDR gives the best performances are at +1 mm and +2 mm of the coupling spacing. The obtained return loss is around 18 dB, which meets the specifications. However, their operating frequency is not accurately operated at 5 GH frequency. The obtained results show when

the coupling spacing is too far or too close between the inhomogeneous CDR and a parallel microstrip lines, the return loss responses will be less than 10 dB. Thus, the suitable coupling needs to be identified between the CDR and parallel microstrip lines.

Table 6
The obtained S-parameters responses (S_{11} and S_{21}) for different spacing between the parallel microstrip lines and the CDR for same port

Spacing (mm)	Same Port		
	Freq (GHz)	***S_{11} (dB)***	***S_{21} (dB)***
-2.5	4.994	-4.257	-2.924
-1	4.998	-8.408	-1.809
0	5.000	-12.829	-1.436
+1	4.998	-18.091	-1.309
+2	4.984	-18.710	-1.516
+3	4.972	-13.297	-2.019
+5	4.954	-6.935	-5.133

The next preliminary study followed by the configuration of the curve of the parallel microstrip lines, which only consider the coupling spacing of +1 mm and +2 mm between the CDR and parallel microstrip lines.

3.2 Curves Configuration of Parallel Microstrip Lines

The next parametric study of the parallel microstrip lines is curved configuration at λ/4 of the wavelength. This is to investigate the effect of curves configuration on the return loss and insertion loss. The different curves configuration at λ/4 wavelength is evaluated for 65˚, 90˚, 155˚, and 165˚ as represented in Figure 2.

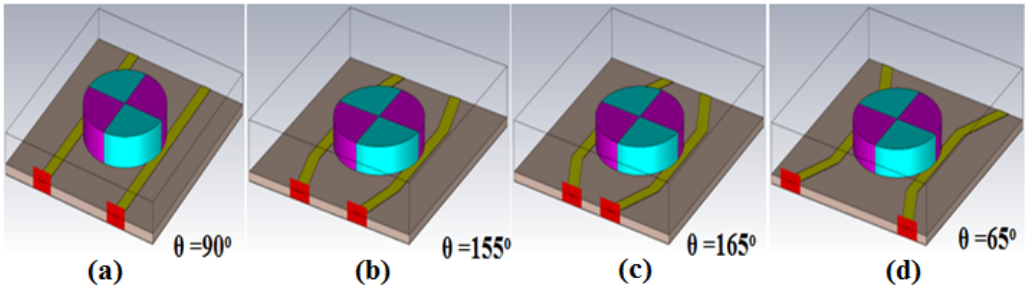

Fig. 2. Parametric study of the different spacing between the parallel microstrip lines

The most common curves configuration is at 90˚, such as mentioned in [36]. The different curve configurations are changed to analyze the best performance of the parallel microstrip lines. The obtained results for this parametric study stated in Table 7.

This parametric study shows the best results are represented by the curve configuration of 90˚ and 155˚. However, only the curve response of 155˚ with +2 mm coupling spacing is shown accurately at 5 GHz frequency. Therefore, the parallel microstrip lines which offers the best performance and can operate at 5 GHz is with +2 mm coupling spacing and 155˚ curves. Therefore, these best parameters will be used in the following investigation that explores the orientation of the angular position for proposed inhomogeneous CDR.

Table 7
The obtained results of the parametric study of the different curve configuration at $\lambda/4$ of the wavelength

Curves Configuration	Different Curved Configurations					
	+1mm (17 mm)			+2mm (19 mm)		
	Freq (GHz)	*S_{11} (dB)*	*S_{21} (dB)*	*Freq (GHz)*	*S_{11} (dB)*	*S_{21} (dB)*
65°	4.982	-4.370	-35.391	5.592	-14.047	-27.980
90°	4.998	-18.091	-1.309	4.984	-18.710	-1.516
155°	5.012	-18.010	-1.721	5.000	-20.538	-2.180
165°	5.012	-13.382	-2.677	4.999	-9.018	-3.415

3.3 Angular Position of the Inhomogeneous Cylindrical Dielectric Resonator

The investigation of the angular position of the inhomogeneous CDR is to find the best angular position that ensures the maximum electromagnetic coupling from the feeding structure to the resonator. The different angular position of the inhomogeneous CDR is evaluated, which are at 0, 10˚, 27.5˚, 30˚ and 55˚ as shown in Figure 3. The orientation of angular position initially refers to the longitudinal axis of the parallel microstrip lines as the references. Subsequently, the orientations of the angular position are changed or rotated in an anticlockwise direction. The findings of the S-parameters (S_{11} and S_{21}) responses for this preliminary study are summarized in Table 8.

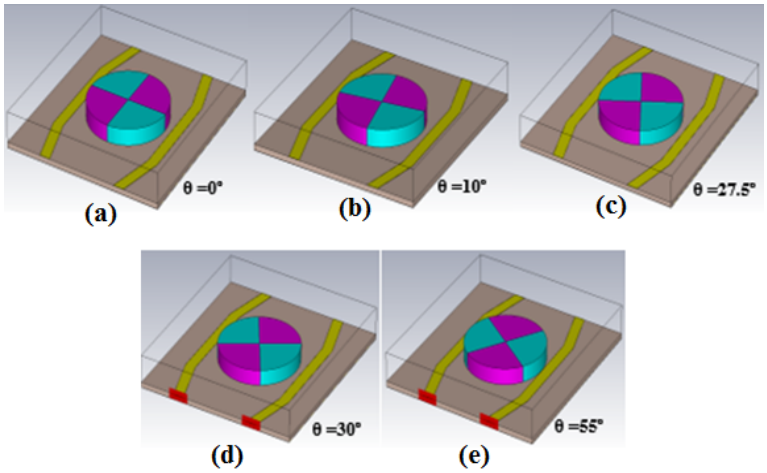

Fig. 3. Parametric study of the different angular position of the inhomogeneous CDR

Table 8
The obtained S-parameters (S_{11} and S_{21}) responses of the parametric study of the different angular position of the inhomogeneous CDR

Angular Position	Curved Configuration (155°)					
	Coupling Spacing (+1 mm)			Coupling Spacing (+2 mm)		
	Freq (GHz)	*S_{11} (dB)*	*S_{21} (dB)*	*Freq (GHz)*	*S_{11} (dB)*	*S_{21} (dB)*
0°	5.012	-18.010	-1.721	5.000	-20.538	-2.180
10°	5.012	-21.250	-1.569	5.000	-16.860	-2.206
27.5°	5.014	-15.573	-1.759	5.002	-14.228	-2.110
30°	5.012	-27.539	-1.852	5.000	-15.765	-2.142
55°	5.014	-17.195	-1.663	5.004	-12.251	-2.120

The obtained S_{11} and S_{21} responses show that there is no significant effect on the resonant frequency as well as the S_{11} and S_{21} performances. However, the orientation without angular position

has the best performances, which are -20.538 dB of S_{11} and -2.180 of S_{21} at 5 GHz frequency. The angular position needs to decide which material out of the two being used has been more influences. Since, the composition of the materials does not have a significant effect on the overall performances, only single or homogeneous CDR is considered. It can be concluded that the best configuration for the CDR consists of 155˚ curved configuration with +2 mm of spacing, which will be used as a dielectric matching component on microwave amplifier.

4. Implementation of the Homogeneous Dielectric Resonator on Microwave Amplifier for Stability Performances

The implementation of the homogeneous DR as the dielectric matching for the microwave amplifier at 5 GHz frequency will incorporate the best configuration which adopted from the previous parametric studies. The stability performances will be evaluated for unconditionally stable (FLC053WG) [37] and conditionally stable (ATF-36077) [38] transistor. The S-parameters responses from both transistors are imported from their datasheet, while the S-parameters responses of the CDR are imported as the 'black box' in ADS software. The use of the radio frequency (RF) choke network is to ensure that the correct direct current (DC) operating voltage is supplied to the active device without allowing the DC supply circuitry to present an improper high-frequency termination to the device. Meanwhile, the DC block prevents DC from flowing to the output and represented by the capacitor [31].

In this article, the dielectric material of the homogeneous CDR is represented by Calcium Copper Titanate (CCTO) with a dielectric permittivity of 34.1991. This homogeneous CDR is placed on top of the substrates between the parallel microstrip lines of 155˚ curved configuration with +2 mm of spacing that acts as dielectric matching on the microwave amplifier. The input and output ports are connected to the vector network analyzer (VNA) through a SMA connector. The circuit is placed in the aluminium box to block the noise and interferences. The S-parameters measurements setup using PNA-X network analyzer is shown in Figure 4.

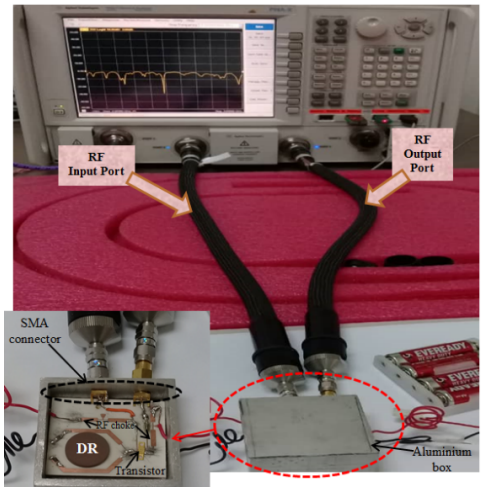

Fig. 4. The S-parameters measurement setup using PNA-X network analyzer

The stability performance of a microwave amplifier is one of the most important characteristics of an amplifier circuit. Therefore, to verify the stability of the transistor, the Rollet's stability, k and stability, μ were observed. The stability represents the values of the stability factor, where it should be more than 1. This condition is necessary for the two-port network to be operated in an

unconditional stable condition. If the value of the stability is less than 1, it shows the transistor is operated in the unstable region. Thus, the microwave amplifier approaches oscillation. In addition, the negative value for these distances of stability also indicates the microwave amplifier resides in an unstable region. This stability, μ can be determined by using (7), whiles the Rollet's stability, K is given in (8) and (9).

$$\mu = \frac{1-|S_{11}|^2}{|S_{22}-conj(S_{11})\times\Delta|+|S_{12}S_{21}|} > 1 \quad (7)$$

$$K = \frac{1-|S_{11}|^2-|S_{22}|^2+|\Delta|^2}{2|S_{12}||S_{21}|} > 1 \quad (8)$$

$$\Delta = |S_{11}||S_{22}| - |S_{12}||S_{21}| < 1 \quad (9)$$

If K>1 and |Δ|<1, the microwave amplifier is considered stable and the necessary condition of stability requirements throughout the selected frequency band is successfully fulfilled. The findings of this investigation are discussed in the next following section.

5. Results and Discussions

The obtained results for the stability analysis performances of CCTO, which is implemented as dielectric matching on microwave amplifier are shown in Figure 5 and Figure 6 for the unconditionally stable (FLC053WG) and conditionally stable (ATF-36077) transistors, respectively. The comparative results of CCTO are observed between the simulation in ADS software (ADS-CCT) and the measurement (VNA-CCTO) for both transistor conditions.

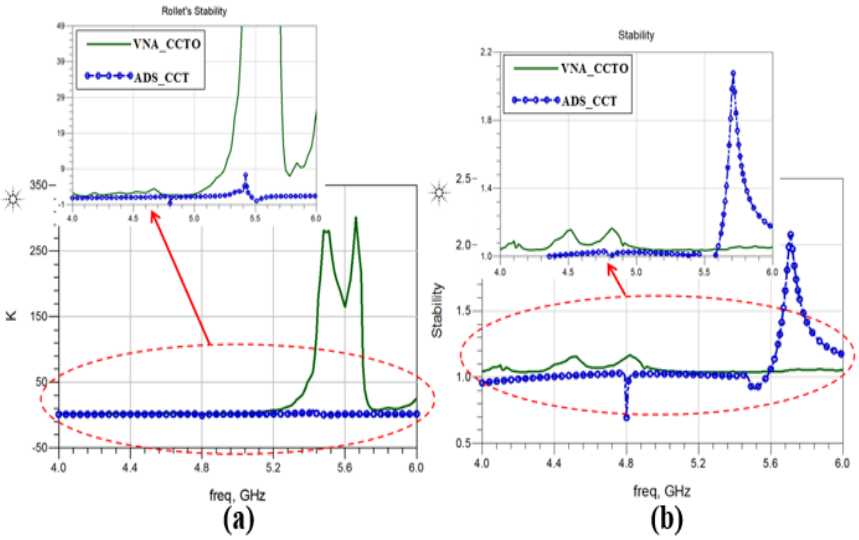

Fig. 5. The stability analysis performances of CCTO for unconditionally stable (FLC053WG) transistor

Figure 5 shows the Rollet's stability, K responses of measurement (VNA_CCTO) is started increases at 5.1 GHz frequency when the CCTO material of CDR is incorporated for the unconditionally stable (FLC053WG) transistor. In between 5.2 GHz and 5.8 GHz frequency, the K is far away from the border of stability condition, which is 1. Meanwhile, the obtained stability performances from the measurements (VNA_CCTO) indicates the overall frequency range is operated in a stable condition within 4.0 GHz until 6.0 GHz frequency.

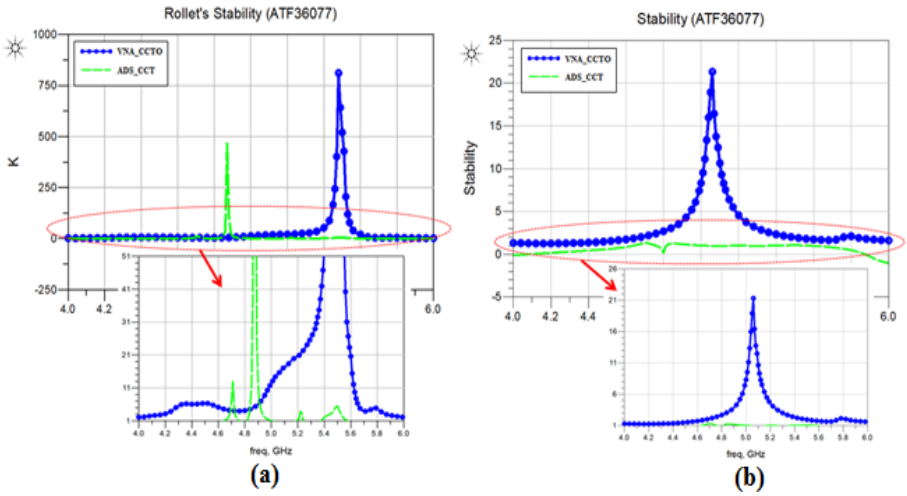

Fig. 6. The stability analysis performances of CCTO for conditionally stable (ATF-36077) transistor

Figure 6 depicts the obtained stability analysis parameter from the simulation (ADS_CCT), which is operated resides in a stable region only at a certain frequency. Like the unconditionally stable (FLC053WG) transistor, the conditionally stable (ATF-36007) transistor also operates in the stable region for the entire frequency range of 4.0 to 6.0 GHz of the measurement (VNA_CCTO) results. The peak of the K responses for the ADS_CCT and VNA_CCTO occurs at 4.9 GHz and 5.5 GHz, respectively. The value of K and stability responses are always related to each other. When the value of K and stability responses are higher than 1, it indicates that the circuits are operated in a stable region and successfully perform as the microwave amplifier.

The differences between the simulation (ADS_CCT) and measurement (VNA_CCTO) may be due to some limitation of the simulator, such as the consideration of the vacuum or aluminium box. Besides that, the tolerance of substrate, dielectric losses, connector, and conductor used to be having a potential to influence the obtained results. However, the implementation of homogeneous DR (CCTO) as the dielectric matching on microwave amplifier shows that it has high potential to perform as the variable frequency mechanism to overcome the issues addressed.

6. Conclusions

This article presents the CDR as dielectric matching on microwave amplifier for unconditional stable and conditional stable transistor at 5 GHz frequency. The characteristics of the CDR, especially for the inhomogeneous CDR, are referred from [29] with the difference of the feeding mechanism used during the preliminary study on microwave amplifier. The parallel microstrip lines at 5 GHz frequency is used as the feeding mechanism for the CDR in this article. Meanwhile, the parametric studies are focused on coupling coefficients and curved configuration between the parallel microstrip lines and the CDR, which affected the resonant frequency in microwave applications, such as an oscillator, amplifier, and filter. This parametric study indicates the best performance of S_{11} and S_{21} of 5 GHz frequency occurs at +2 mm spacing distance with 155˚ of curved configuration, which is -20.538 dB and -2.142 dB, respectively. This curve position configuration improves the performance of parallel inhomogeneous CDR by 9.77%. Then, the orientation of the angular position is analyzed, especially for inhomogeneous CDR. The obtained results show the best performance at 5 GHz is without the angular position, which indicates the orientation of the angular position can be ignored. All parameters of the preliminary studies are based on the conventional and empirical investigation. Therefore, the implementation of the CDR is represented by homogeneous CDR as the dielectric

matching on microwave amplifier. The comparative results of CCTO are observed between the simulation via ADS software and the measurements for unconditionally stable and conditionally stable transistors. As results, the issues about the stability and matching techniques on microwave amplifier are successfully overcome by incorporating homogeneous CDR as the dielectric matching. The homogeneous CDR that representing by CCTO is successfully working as the variable frequency mechanism for unconditionally stable and conditionally stable transistor at 5 GHz frequency in maintaining their stability performances.

Acknowledgement
The authors thanks to Universiti Malaysia Perlis (UniMAP) for the funding and support of the research work under Research Materials Fund (RESMATE), 9001-00627. The members of Faculty of Electronic Engineering Technology, UniMAP and Universiti Sains Malaysia (USM) are also specially thanks for their helps and kindness.

References

[1] Eroglu, A. "Stabilization of Class E amplifiers with a diode network." *AEU – International Journal of Electronics and Communications* 64, no. 3 (2010): 224-230. https://doi.org/10.1016/j.aeue.2008.11.009
[2] Han, Y., and Perreault, D. J. "Analysis and design of high efficiency matching networks." *IEEE Transaction on Power Electronics* 21, no. 5 (2006): 1484-1491. https://doi.org/10.1109/TPEL.2006.882083
[3] Grebennikov, A. (2015). *Chapter 6 - Stabilization circuit technique*. RF and microwave power amplifier design, New York, NY, USA: McGraw-Hill Professional Engineering, Page 426-450.
[4] Pozar, D. M. (2005). *Chapter 11 - Microwave amplifier design*. Microwave Engineering, 3rd Ed. New York: Wiley, Page 536-572.
[5] Khabbaz, A., Sobhi, J., and Daei Koozehkanani, Z. "A sub-mW 2.9-dB noise figure Inductor-less low noise amplifier for wireless sensor network applications." *AEU – International Journal of Electronics and Communications* 93, (2018): 132–139. https://doi.org/10.1016/j.aeue.2018.06.013
[6] Lin, Y.-S., Wang, C.-C., and Lee, J.-H. "Design and implementation of a 1.9-22.5 GHz CMOS wideband LNA with dual-RLC-branch wideband input and output matching networks." *Microwave and Optical Technology Letters* 56, no. 3 (2014): 677–684. https://doi.org/10.1002/mop.28186
[7] Vimal, S., and Maheshwari, M. "Design and performance improvement of a low noise amplifier with different matching techniques and stability network." *International Journal of Engineering Research & Science (IJOER)* 2, no. 3 (2016): 1-10.
[8] Alimenti, F., Virili, M., Mezzanotte, P., Roselli, L., Rericha, V., Pokorny, M., Iorio, F., Gaddi, R., and Schepens, C. "A RF-MEMS based tuneable matching network for 2.45 GHz discrete-resizing CMOS power amplifiers." *Radioengineering* 23, no. 1 (2014): 328-337.
[9] Fabbro, P. A. D., and Kayal, M. "RF power amplifier employing a frequency tunable impedance matching network based on coupled inductors." *Electronic Letters* 44, no. 19 (2008): 1131 -1132. https://doi.org/10.1049/el:20089196
[10] Hoarau, C., Corrao, N., Arnould, J.-D., Ferrari, P., and Xavier, P. "Complete design and measurement methodology for a tunable RF impedance-matching network. "*IEEE Transaction on Microwave Theory and Technology* 56, no. 11 (2008): 2620–2627. https://doi.org/10.1109/TMTT.2008.2006105
[11] Wong, Y. C., Sarban Singh, R. S., Ahmad Radzi, S. B., and Abdul Hamid, N. B. "Tunable impedance matching network with wide impedance coverage for multi frequency standards RF front-end." *AEU - International Journal of Electronics and Communications* 82, (2017): 74–82. https://doi.org/10.1016/j.aeue.2017.08.004
[12] Iyer, M. and Shanmuganantham, T. "Design of LNA for C band applications." In *IEEE International Conference on Circuits and Systems (ICCS)*, p. 211-214. 2017. https://doi.org/10.1109/ICCS1.2017.8325992
[13] Veeranjaneyulu, M., and Anuradha Thiruvananthapuram, India,, B. "Design & simulation of radio frequency power amplifiers for high efficiency and without affecting linearity." *International Journal on Recent and Innovation Trends in Computing and Communication* 4, no. 8 (2016): 46-49.
[14] Madhura, P. J., and Savita, B. B. "Efficient designing techniques for low noise amplifier." In 22nd IRF International Confonference, Pune, India, p. 106-108. 2015.
[15] Fallahnejad, M., and Alireza, K. "Design of low noise amplifiers at 10 GHz and 15 GHz for wireless communications systems." *IOSR Journal of Electrical and Electronic Engineering (IOSR-JEEE)* 9, no. 5 (2014): 47-53. https://doi.org/10.9790/1676-09544753

[16] Fallahnejad, M., Yasaman, N., and Alireza, K. "Design and simulation of low noise amplifier at 10 GHz by using GaAs High Electron Mobility transistor." *IOSR Journal of Electrical and Electronic Engineering (IOSR-JEEE)* 10, no. 5 (2015): 29-34.
[17] Lim, Y., Tang, H., Lim, S., and Park, J. "An adaptive impedance-matching network based on a novel capacitor matrix for wireless power transfer." *IEEE Transaction on Power Electronics* 29, no. 8 (2014): 4403-4413. https://doi.org/10.1109/TPEL.2013.2292596
[18] Senthilkumar, D., Uday, P. K., and Santosh, J. "Design and comparison of different matching techniques for low noise amplifier circuit." *International Journal Engineering Research and Applications (IJERA)* 3, no. 1 (2013): 403-408.
[19] Yu-na, S., and Geng, L. "Design of a low noise amplifier of RF communication receiver for mine." In *IEEE Symposium on Electrical & Electronics Engineering (EEESYM),* Kuala Lumpur, Malaysia, p.125-127. 2012. https://doi.org/10.1109/EEESym.2012.6258604
[20] Gao, S. Wang, Z., and Chan-Wang, P. "A novel RF tunable impedance matching network for correcting the tested result deviation from simulated result." In *Proceedings of 2010 IEEE Asia-Pacific Conference on Applied Electromagnetics (APACE 2010)*, Port Dickson, Negeri Sembilan, Malaysia, p.1-4. 2010.
[21] Fuzy, C., and Zolomy, A. "Design of broadband complex impedance-matching networks and their applications for broadbanding microwave amplifiers." In *18th International Conference on Microwave Radar and Wireless Communications (MIKON)*, Vilnius, Lithuania, p.1-4. 2010.
[22] Boughariou, M., Fakhfakh, M., and Loulou, M. "Design and optimization of LNAs through the scattering parameters." In *15th IEEE Mediterranean Electrotechnical Conference (MELECON)*, Valletta, Malta, p.764-767. 2010. https://doi.org/10.1109/MELCON.2010.5475973
[23] Khah, S. K., Singh, P., Rabra, S., Saxena R., and Chakarvarty, T. "Broadband impedance matching technique for microwave amplifiers." In *IEEE Applied Electromagnetics Conference (AEMC)*, Kolkata, India, p.1-4. 2007. https://doi.org/10.1109/AEMC.2007.4638055
[24] Collado, A., Ramirez, F., and Suarez, A. "Analysis and stabilization tools for microwave amplifiers." In *IEEE MTT-S Int. Microwave Symposium Digest*, Fort Worth, TX, USA, p.945-948. 2004.
[25] Ibrahim, A. B., Kahar, N. H., Hanafi, H. F., Ariffin S. A., and Abas, A. "A New Cascode Low Noise Amplifier (LNA) with Double Feedback Technique Architecture for Long Term Evolution (LTE) Application." *Journal of Advanced Research in Applied Mechanics* 77, no. 1 (2021): 1-10.
[26] Jain, A., Hannurkar, P. R., Pathak, S. K., Biswas, A., and Srivastva, M. "Improved performance of two-way power divider using dielectric resonator." *Microwave and Optical Technology Letters* 56, no. 4 (2014): 858-861. https://doi.org/10.1002/mop.28236
[27] Su, Y., Zhao, H. L., Liu, X. F., and Huang, L. H. "Design of the dielectric resonator oscillator with buffer amplifier." *Advanced Materials Research* 433-440, (2012): 4536–4540. https://doi.org/10.4028/www.scientific.net/AMR.433-440.4536
[28] Yan, G. "The design of the Ku band dielectric resonator oscillator." In *International Conference on Electronic Packaging Techology & High Density Packaging (ICEPT-HDP)*, Shanghai, China, p.1-3. 2008.
[29] Olokede, S. S., Zaki, S. B. B. M., Mahyuddin, N. M., Ain, M. F., and Ahmad, Z. A. "Design of a negative conductance dielectric resonator oscillator for X-band applications." *Radioelectronics and Communications Systems* 60, no. 9 (2017): 413–422. https://doi.org/10.3103/S0735272717090059
[30] Ullah, U. (2016). *Study of inhomogeneous dielectric resonators for linearly/circularly polarized microwave antenna applications*. Universiti Sains Malaysia, MALAYSIA (PhD Thesis).
[31] Ullah, U., Ali, W. F. F. W., Ain, M. F., Mahyuddin, N. M., and Ahmad, Z. A. "Design of a novel dielectric resonator antenna using MgTiO3-CaTiO3 for wideband applications." *Materials and Design* 85, (2015): 396-403. https://doi.org/10.3103/S0735272717090059
[32] Ullah, U., Ain, M. F., Othman, M., Zubir, I., Mahyuddin, N. M., Ahmad, Z. A., and Abdullah, M. Z. "A novel multi-permittivity cylindrical dielectric resonator antenna for wideband applications." *Radioengineering* 23, (2014): 1071-1076.
[33] Rogers Cooperation. (2011). RO4000 Series High Frequency Circuit Materials, Advanced Connectivity Solutions.
[34] Mahyuddin, N. M. (2006). *Design and implementation of a 10 GHz dielectric resonator oscillator*. Universiti Sains Malaysia, MALAYSIA (Master Thesis).
[35] Marulanda, J. I., Lina. R. A. A., Carvalho, M. C. R., Almeida, A. F. L., Sombra, A. B. S., and Demenicis, L. S. "Characterization of dielectric properties of screen-printed MgTiO3-CaTiO3 composite thick films in the microwave frequency range." In *IEEE MTT-S International Microwave and Optoelectronics Conference (IMOC),* Belem, Brazil, p.211-214. 2009. https://doi.org/10.3103/S0735272717090059

[36] Mahyuddin, N. M., Ain, M. F., Hassan, S. I. S. and Singh, M. "A 10 GHz PHEMT dielectric resonator oscillator." In *Proceedings of the IEEE International RF and Microwave Conference.*, Putrajaya, Malaysia, p. 26-30. 2006. https://doi.org/10.3103/S0735272717090059
[37] Fujitsu Semiconductor. (1998). *FLC053WG Datasheets: C-band Power GaAs FETs*.
[38] Hewlett-Packard. (1997) *2-18 GHz Ultra Low Noise Pseudomorphic HEMT (ATF-36077)*.